

Surface-Enhanced Raman Excitation Spectroscopy of a Single Rhodamine 6G Molecule

Jon A. Dieringer, Kristin L. Wustholz, David J. Masiello, Jon P. Camden, Samuel L. Kleinman, George C. Schatz, and Richard P. Van Duyne*

Department of Chemistry, Northwestern University, Evanston, Illinois 60208

Received October 15, 2008; E-mail: vanduyne@northwestern.edu

Abstract: The surface-enhanced Raman excitation profiles (REPs) of rhodamine 6G (R6G) on Ag surfaces are studied using a tunable optical parametric oscillator excitation source and versatile detection scheme. These experiments afford the ability to finely tune the excitation wavelength near the molecular resonance of R6G (i.e., ~500–575 nm) and perform wavelength-scanned surface-enhanced Raman excitation measurements of a single molecule. The ensemble-averaged surface-enhanced REPs are measured for collections of molecules on Ag island films. The relative contributions of the 0–0 and 0–1 vibronic transitions to the surface-enhanced REPs vary with vibrational frequency. These results highlight the role of excitation energy in determining the resonance Raman intensities for R6G on surface-enhancing nanostructures. Single-molecule measurements are obtained from individual molecules of R6G on Ag colloidal aggregates, where single-molecule junctions are located using the isotope-edited approach. Overall, single-molecule surface-enhanced REPs are narrow in comparison to the ensemble-averaged excitation profiles due to a reduction in inhomogeneous broadening. This work describes the first Raman excitation spectroscopy studies of a single molecule, revealing new information previously obscured by the ensemble.

Introduction

The vibrational signature of individual molecules can be measured using single-molecule surface-enhanced Raman spectroscopy (SMSERS), a technique first described in 1997 by the groups of Nie and Kneipp.^{1,2} Over a decade since its discovery and the emergence of numerous SMSERS investigations,^{3–11} fundamental mechanistic questions remain. For example, much attention is focused on characterizing the relative importance of the electromagnetic, chemical, and resonance Raman enhancement mechanisms that are responsible for single-molecule sensitivity. In the original SMSERS reports, the enhancement factor (EF) was estimated to be 10^{14} – 10^{15} by comparing the measured SER cross-section of rhodamine 6G (R6G) on Ag nanoaggregates ($\sim 10^{-15}$ cm²) to a typical Raman scattering cross-section ($\sim 10^{-30}$ cm²).¹ However, the absolute Raman cross-section of R6G on molecular resonance ($\lambda_{\text{ex}} = 532$ nm) was recently determined to be $\sim 10^{-23}$ cm² using femtosecond

stimulated Raman spectroscopy.¹² As a consequence, the resonance Raman contribution accounts for as much as 10^7 of the previously predicted $\sim 10^{15}$ enhancement in the R6G/Ag system, assuming the Raman cross-section in solution and on the surface are similar. Therefore, the remaining 10^8 enhancement is attributable to surface effects. Consistent with this work, recent computational studies have demonstrated the feasibility for single-molecule detection on the molecular resonance of R6G through a combination of electromagnetic enhancement of 10^8 and the measured Raman cross-section of R6G.¹³ Experimental investigations have likewise demonstrated single-molecule sensitivity using excitation at the molecular resonance of R6G with an isotope-edited approach.⁴ Ultimately, these studies establish that an electromagnetic mechanism (EM) EF of 10^8 is all that is required for the observation of SMSERS from the R6G/Ag nanoaggregate system, provided that excitation occurs at the molecular resonance.¹⁴

When excitation occurs away from molecular resonance, the contributions of resonance Raman and surface effects to SMSERS activity are less understood. Previous SMSERS studies on the R6G/Ag system have employed various excitation wavelengths.^{1,9,15} For example, Vosgröne and Meixner measured SER spectra of R6G at different excitation wavelengths (i.e., $\lambda_{\text{ex}} = 632.8, 532.0, 514.4, 488.0,$ and 457.9 nm) on samples with varied dye concentration, demonstrating that SER spectra obtained at 532 nm provided the maximum sensitivity ($\sim 10^{-13}$

- (1) Nie, S. M.; Emory, S. R. *Science* **1997**, *275*, 1102.
- (2) Kneipp, K.; Wang, Y.; Kneipp, H.; Perelman, L. T.; Itzkan, I.; Dasari, R.; Feld, M. S. *Phys. Rev. Lett.* **1997**, *78*, 1667.
- (3) Bizzarri, A. R.; Cannistraro, S. *Phys. Rev. Lett.* **2005**, *94*.
- (4) Dieringer, J. A.; Lettan, R. B.; Scheidt, K. A.; Van Duyne, R. P. *J. Am. Chem. Soc.* **2007**, *129*, 16249.
- (5) Doering, W. E.; Nie, S. M. *J. Phys. Chem. B* **2002**, *106*, 311.
- (6) Goulet, P. J. G.; Aroca, R. F. *Anal. Chem.* **2007**, *79*, 2728.
- (7) Haran, G. *Isr. J. Chem.* **2004**, *44*, 385.
- (8) Le Ru, E. C.; Meyer, M.; Etchegoin, P. G. *J. Phys. Chem. B* **2006**, *110*, 1944.
- (9) Michaels, A. M.; Nirmal, M.; Brus, L. E. *J. Am. Chem. Soc.* **1999**, *121*, 9932.
- (10) Moore, A. A.; Jacobson, M. L.; Belabas, N.; Rowlen, K. L.; Jonas, D. M. *J. Am. Chem. Soc.* **2005**, *127*, 7292.
- (11) Xu, H. X.; Aizpurua, J.; Käll, M.; Apell, P. *Phys. Rev. E* **2000**, *62*, 4318.

- (12) Shim, S.; Stuart, C. M.; Mathies, R. A. *ChemPhysChem* **2008**, *9*, 697.
- (13) Camden, J. P.; Dieringer, J. A.; Wang, Y. M.; Masiello, D. J.; Marks, L. D.; Schatz, G. C.; Van Duyne, R. P. *J. Am. Chem. Soc.* **2008**, *130*, 12616.
- (14) Le Ru, E. C.; Blackie, E.; Meyer, M.; Etchegoin, P. G. *J. Phys. Chem. C* **2007**, *111*, 13794.
- (15) Vosgröne, T.; Meixner, A. *J. ChemPhysChem* **2005**, *6*, 154.

M).¹⁵ Le Ru et al. showed that single-molecule SERS was observed with a SER cross-section of $\sim 10^{-17}$ cm², corresponding to an EF $\approx 10^9$ at $\lambda_{\text{ex}} = 633$ nm.¹⁴ These investigations suggest that the maximum SMSERS intensity occurs at the molecular resonance of R6G and that single molecules are observable far from resonance (e.g., at 633 nm). Yet, the nature of the excitation-wavelength dependence of SMSERS is still not well characterized.¹⁶ Prior studies were not performed on the *same* nanoparticle aggregate nor the *same* molecule and have been limited to fixed-frequency laser sources. In this work, we seek to characterize the resonance Raman contributions to SMSERS intensity about the molecular resonance. The surface-enhanced Raman excitation profiles (REPs) of a single R6G molecule on Ag nanoparticle aggregates are measured using a tunable optical parametric oscillator excitation source and versatile detection scheme. These experiments afford the ability to finely tune the excitation wavelength near the molecular resonance of R6G (i.e., ~ 500 – 575 nm) and perform wavelength-scanned SMSERS measurements of the same molecule.

Experimental Section

Syntheses. Following the procedure of Lee and Miesel,¹⁷ 90 mg of AgNO₃ (Aldrich) was dissolved in 500 mL of deionized water (Millipore Milli-Q, 18.2 M Ω ·cm) in a 1 L flask. After bringing the solution to a boil, 10 mL of a 1% sodium citrate (Aldrich) solution was added while stirring rapidly. The solution was boiled for 30 min, during which the solution first turned transparent yellow and then finally opaque gray. After boiling, the nanoparticle solution was cooled to room temperature and diluted to a final volume of ~ 420 mL. The majority of the nanoparticles prepared using this technique are spherical with an average diameter of 35 nm, but prisms, platelets, disks, and rods of various sizes were also present. The synthesis of rhodamine 6G-*d*₄ (R6G-*d*₄) is based on the conditions given by Zhang et al.¹⁸ and is reported elsewhere.⁴

SERS Sample Preparation and Characterization. Silver island films (AgIF) were prepared by electron beam evaporation (Kurt J. Lesker, Co. AXXIS) of 6 nm Ag (Kurt J. Lesker, Co., 99.999%) onto piranha-cleaned, base-treated glass coverslips at a rate of 2.0 Å·s⁻¹. The island films were incubated in ethanolic solution containing either 10⁻⁴ M R6G (Aldrich) or 10⁻³ M benzenethiol (Aldrich) for 3 h, rinsed with ethanol, and dried. The R6G/AgIF sample was mounted in a custom designed flow cell for environmental control and exposed to dry N₂. Corresponding samples for surface absorbance measurements of R6G on Ag were prepared using 200 nm Ag films under the same deposition and incubation conditions. Surface absorbance measurements were made on a photodiode-array spectrophotometer (HP 8452A) equipped with an integrating sphere (Labsphere RSA-HP-84) for specular reflectance spectroscopy.

SMSERS Sample Preparation. A 10 mL solution of chemically prepared Ag nanoparticles (10⁻⁹ M) was treated with 1 mL of a 50:50 mixture containing R6G (5×10^{-10} M) and R6G-*d*₄ (5×10^{-10} M) such that ~ 0.5 R6G and 0.5 R6G-*d*₄ were adsorbed per nanoparticle (final concentrations after mixing). Statistically, there is nominally one molecule per nanoparticle, with equal probability of it being R6G or R6G-*d*₄, although the total number adsorbed will deviate according to the Poisson distribution. The nanoparticles were diluted by 50% with 20 mM NaCl (final concentration in solution 10 mM) to cause aggregation, but not precipitation.¹⁹ A

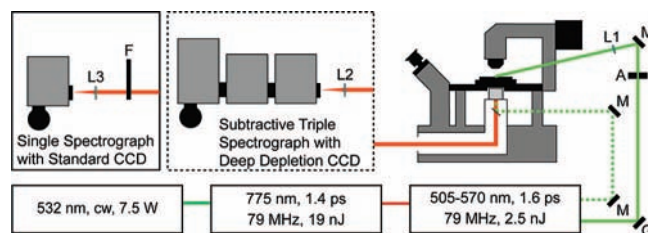


Figure 1. Instrumental diagram. Excitation is provided by a series of lasers generating 505–600 nm. For ensemble-averaged studies the optical path is indicated by a dashed line. The laser is incident on the sample in the epi configuration and Raman scattering is analyzed on a three-stage, subtractive monochromator equipped with a CCD. For single-molecule studies, the optical path is indicated by a solid line. The laser is spectrally filtered by a grating (G) and aperture (A) combination and is focused by L1 ($f = 400$ mm) at grazing incidence. Inelastic Raman scattering is sent through a filter wheel (F) and analyzed on a single channel monochromator equipped with a CCD.

10 μ L aliquot of this solution was drop-coated on piranha-cleaned, base-treated glass coverslips to immobilize the nanoparticles. Samples were mounted in a custom-designed flow cell for environmental control and exposed to dry N₂.

Wavelength-Scanned SERS Instrumentation. Samples were illuminated by laser excitation from a synchronously pumped, periodically poled, intracavity-doubled optical parametric oscillator (Coherent Mira-OPO, 80 MHz, ps-configuration) pumped by a mode-locked Ti:Sapphire oscillator at 775 nm (Spectra-Physics Tsunami, 80 MHz, ps-configuration). A diode-pumped solid-state laser (Spectra-Physics Millennia, 532 nm) was used to drive the oscillator. The samples were illuminated with ~ 500 – 575 nm light in an epi configuration such that both excitation and collection of the inelastic Raman scattering were performed with an oil-immersion objective equipped with a variable numerical aperture (NA) iris set to NA = 0.5 (Nikon, Plan Fluor 100X, oil, iris) on an inverted microscope (Nikon TE300). The signal was analyzed with a triple spectrograph (Acton) consisting of two 1/3 m spectrographs in subtractive mode with 600 groove·mm⁻¹ gratings blazed at 500 nm, a 1/2 m dispersive stage with a 1200 groove·mm⁻¹ grating blazed at 500 nm, and detected by a LN₂-cooled CCD camera (Princeton Instruments Spec-10 400BR). Typical power densities (P_{ex}) and integration times (t_{ac}) were 150 W·cm⁻² and 20 s, respectively. A schematic of the instrument is presented in Figure 1, wherein the beam path is designated by the dashed line.

Wavelength-Scanned SMSERS Instrumentation. The instrumentation for the single-molecule experiments is identical to ensemble-averaged experiments with the following exceptions (Figure 1, solid lines). A 1200 groove·mm⁻¹ grating was inserted into the beam and the first-order diffraction was filtered at a distance of ~ 3 m by a 1 mm aperture to narrow the excitation bandwidth, broaden the pulse duration to limit sample damage, and generate a tunable system not relying on excitation interference filters. Excitation at grazing incidence produced a weakly focused elliptical spot of $\sim 1 \times 2$ mm². A holographic notch filter (Kaiser, 532 nm) was placed in the microscope to reject excitation light such that visual observation of the inelastic scattering was observable by eye and appeared diffraction limited. In order to reject Rayleigh scattering of the tunable excitation, the 532 nm notch filter was removed and a filter wheel containing a series of appropriate filters (Kaiser Optical, 506 nm notch; Semrock, 514 nm long-pass; Chroma, 532 nm long-pass) was placed before the spectrograph. The combination of these filters enabled continuous measurements between 505–518 and 528–540 nm. The inelastically scattered light was analyzed with a 1/3 m imaging spectrometer containing a 1200 groove·mm⁻¹ grating blazed at 500 nm (Acton 300i) and equipped with a LN₂-cooled CCD camera (Princeton Instruments Spec-10 400B). Individual diffraction-limited spots were centered on the entrance slit of the spectrograph, and Raman spectra were collected as a function of wavelength. Typical P_{ex} and t_{ac} for single-

(16) Camden, J. P.; Dieringer, J. A.; Zhao, J.; Van Duyne, R. P. *Acc. Chem. Res.* **2008**, *41*, 1653.

(17) Park, S. K.; Lee, C. K.; Min, K. C.; Lee, N. S. *Bull. Kor. Chem. Soc.* **2004**, *25*, 1817.

(18) Zhang, D. M.; Xie, Y.; Deb, S. K.; Davison, V. J.; Ben-Amotz, D. *Anal. Chem.* **2005**, *77*, 3563.

(19) Meyer, M.; Le Ru, E. C.; Etchegoin, P. G. *J. Phys. Chem. B* **2006**, *110*, 6040.

molecule experiments were $0.050 \text{ W} \cdot \text{cm}^{-2}$ and 10 s, respectively. These parameters were carefully optimized to prevent photodegradation of the single-molecule system. Triplicate SMSER spectra were obtained at each excitation wavelength in order to measure the average intensity and standard deviation from the mean. Localized surface plasmon resonance (LSPR) spectra of the active SMSERS sites were measured on the microscope using white-light illumination through a dry dark-field condenser (Nikon, NA 0.7–0.95). A low-dispersion grating ($300 \text{ groove} \cdot \text{mm}^{-1}$) was inserted to collect the broadband spectrum. The LSPR and SMSER spectra originated from the same diffraction-limited spot, based on comparison of images of the inelastic and elastic scattering.

Discrete-Dipole Approximation. Numerical continuum-electrodynamics calculations were performed with DDSCAT 6.1²⁰ to simulate electric-dipole scattering from a model SMSERS active T-shaped Ag nanoparticle dimer studied elsewhere.¹³ Modification of the discrete-dipole approximation (DDA) method to retain the scattered electric-dipole fields allowed investigation of scattering and absorption cross-sections of the nanoaggregate, as well as the resultant electric-field distributions and hot spots as a function of incident wavelength, polarization, material dielectric behavior, and target discretization. Particular scrutiny was made in the spectral region between 530 and 535 nm, near the experimentally relevant molecular-electronic resonance of R6G. Parameters for the calculation included (1) the Ag dielectric data of Palik,²¹ (2) representation of the nanoparticle dimer by a finite collection of polarizable points spaced 1 nm apart, and (3) the same incident polarization and propagation direction defined previously.¹³ While these purely classical electrodynamics calculations do not incorporate the chromophore or its coupling to the Ag dimer, they qualitatively describe the dynamical electric-field scattering effects of the nanoparticle structure itself.

Data Analysis. The observed Raman frequencies were measured by calibrating to a cyclohexane standard.²² Surface-enhanced Raman intensities were calculated using custom software written in Matlab R14 (Mathworks). Individual modes were fit to Lorentzian functions using unconstrained nonlinear minimization built into *fminsearch*. Absorbance spectra and surface-enhanced REPs were fit to Gaussian or Lorentzian functions in PeakFit 4.12 (SeaSolve) by minimizing the residuals.

Results and Discussion

Surface-Enhanced Raman Spectroscopy of R6G. The surface-enhanced resonance Raman spectrum of R6G on a Ag island film obtained using 532 nm excitation from a Millennia X laser ($P_{\text{ex}} = 2.0 \text{ kW} \cdot \text{cm}^{-2}$, $t_{\text{ac}} = 0.1 \text{ s}$) is presented in Figure 2a. A broad background is observed, originating from continuum emission of the substrate (i.e., the SERS background) and/or fluorescence from R6G directly adsorbed to glass between silver islands. Prominent Raman modes at 1647, 1504, 1360, 771, and 610 cm^{-1} are observed, in agreement with previous experimental^{1,23} and theoretical investigations.^{24–26}

In resonance Raman spectroscopy, it is well-known that the REPs are closely related to the molecular absorbance.^{27–29} The

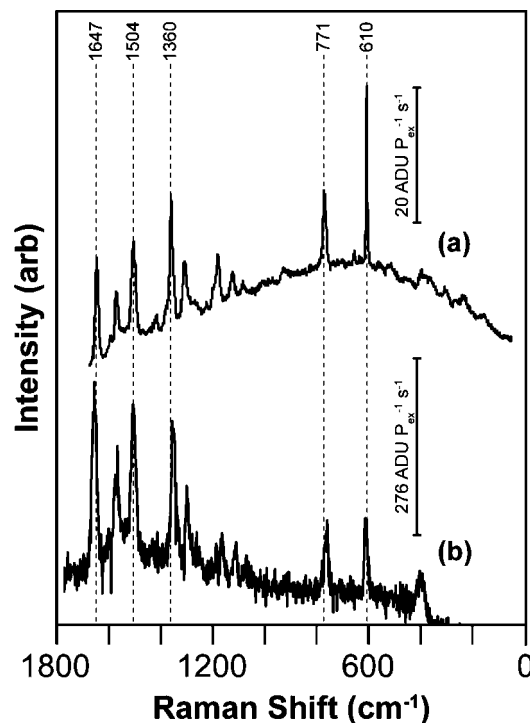


Figure 2. Surface-enhanced Raman spectra of R6G on silver obtained using 532-nm excitation. (a) Ensemble-averaged surface-enhanced resonance Raman obtained on AgIF ($P_{\text{ex}} = 2.0 \text{ kW} \cdot \text{cm}^{-2}$, $t_{\text{ac}} = 0.1 \text{ s}$) and (b) single-molecule surface-enhanced resonance Raman spectrum obtained on colloidal Ag aggregate ($P_{\text{ex}} = 0.050 \text{ W} \cdot \text{cm}^{-2}$, $t_{\text{ac}} = 30 \text{ s}$).

absorbance of R6G on Ag was measured using specular reflectance in an integrating sphere. In ethanolic solution, R6G exhibits an absorbance maximum (E_{max}) at 18986 cm^{-1} (526.7 nm) with a vibronic shoulder at 19960 cm^{-1} (501.0 nm). The full-width-half-maximum (fwhm) of each peak is 974 and 1997 cm^{-1} , respectively. The difference in energy between the absorbance maximum (0–0 transition) and the vibronic sideband (0–1 transition) does not correspond to a particular vibrational mode of R6G. Moreover, the 0–1 transition is broad, indicating that vibronic coupling occurs to multiple modes. When adsorbed to Ag, R6G exhibits a surface absorbance that is well described by a sum of two Gaussian functions (Figure 3a). The best fit corresponds to maxima and fwhm of $E_{\text{max}} = 18409 \text{ cm}^{-1}$ (543.2 nm), $\text{fwhm} = 1004 \text{ cm}^{-1}$ and $E_{\text{max}} = 19246 \text{ cm}^{-1}$ (519.6 nm), $\text{fwhm} = 1822 \text{ cm}^{-1}$, for the 0–0 and 0–1 transitions, respectively. Consistent with previous observations, the absorbance of R6G on Ag exhibits a red-shift relative to solution.³⁰

Recently, Shim et al. measured the absolute resonance Raman cross-section of R6G using femtosecond stimulated Raman spectroscopy and predicted corresponding REPs using a resonance Raman modeling program.¹² As the vibrational frequency increased, the REP intensity shifted from the 0–0 transition to the 0–1 transition. For example, while the 604 cm^{-1} mode exhibited a single band at the absorbance maximum (i.e., 0–0 transition), the 1642 cm^{-1} mode exhibited two well-resolved bands corresponding to the 0–0 and 0–1 transitions. Therefore, the surface-enhanced REPs of R6G should contain superpositions of the measured surface absorbance transitions, weighted differentially for each vibrational mode.

(20) Draine, B. T.; Flatau, P. J. *J. Opt. Soc. Am. A* **1994**, *11*, 1491.

(21) Palik, E. D. *Handbook of Optical Constants of Solids*; Academic Press: New York, 1985.

(22) McCreery, R. L. *Raman Spectroscopy for Chemical Analysis*; Wiley-Interscience: New York, 2000; Vol. 157.

(23) In our previous work on R6G, we reported vibrational frequencies that were self-consistent but had a systematic calibration offset of $\sim 11 \text{ cm}^{-1}$.

(24) Guthmuller, J.; Champagne, B. *ChemPhysChem* **2008**, *9*, 1667.

(25) Jensen, L.; Schatz, G. C. *J. Phys. Chem. A* **2006**, *110*, 5973.

(26) Watanabe, H.; Hayazawa, N.; Inouye, Y.; Kawata, S. *J. Phys. Chem. B* **2005**, *109*, 5012.

(27) Myers, A. B. *J. Raman Spectrosc.* **1997**, *28*, 389.

(28) Hildebrandt, P.; Stockburger, M. *J. Phys. Chem.* **1984**, *88*, 5935.

(29) Clark, R. J. H.; Franks, M. L.; Turtle, P. C. *J. Am. Chem. Soc.* **1977**, *99*, 2473.

(30) Zhao, J.; Jensen, L.; Sung, J. H.; Zou, S. L.; Schatz, G. C.; Van Duyne, R. P. *J. Am. Chem. Soc.* **2007**, *129*, 7647.

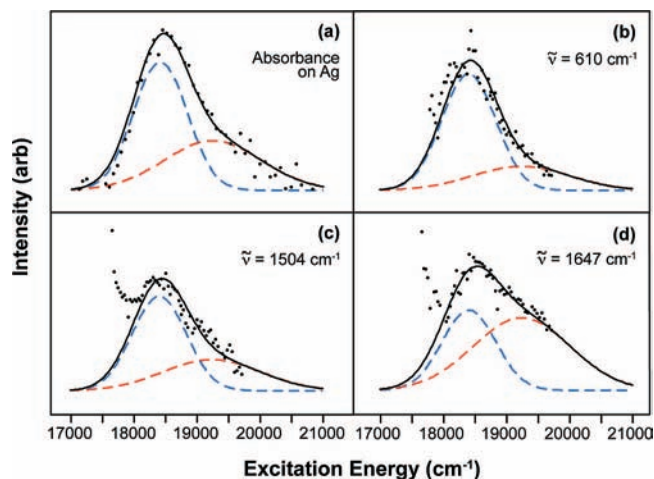


Figure 3. Absorbance of R6G on Ag (a). Ensemble-averaged surface-enhanced Raman excitation profiles of different Raman modes of R6G on AgIF. (b) $\nu = 610$, (c) 1504, and (d) 1647 cm^{-1} ($P_{\text{ex}} \approx 150 \text{ W} \cdot \text{cm}^{-2}$, $t_{\text{ac}} = 20 \text{ s}$). The black solid lines represent a fit of the data (points) to a sum of two Gaussians. The dashed lines correspond to the deconvolution of the overall fit, demonstrating relative contributions from the 0–0 and 0–1 vibronic transitions of R6G on Ag ($E_{\text{max}} = 18409 \text{ cm}^{-1}$, fwhm = 1004 cm^{-1} and $E_{\text{max}} = 19246 \text{ cm}^{-1}$, fwhm = 1822 cm^{-1}).

Surface-enhanced REPs for R6G on AgIF were measured using an optical microscope coupled to a tunable excitation source and detection system (Figure 1, dashed lines). In this work, three prominent vibrational modes of R6G (i.e., 1647, 1504, and 610 cm^{-1}) were chosen for analysis since they represent behavior in different spectral regimes (from large to modest Raman shift) and have demonstrated interesting REP characteristics.¹² The surface-enhanced REPs of R6G on AgIF under dry N_2 are presented in Figure 3b–d. The excitation profiles were fit to a sum of two Gaussians, where E_{max} and fwhm were set to the deconvoluted surface absorbance transitions. That is, $E_{\text{max}} = 18409 \text{ cm}^{-1}$ (543.2 nm), fwhm = 1004 cm^{-1} and $E_{\text{max}} = 19246 \text{ cm}^{-1}$ (519.6 nm), fwhm = 1822 cm^{-1} . The surface-enhanced REP for the 610 cm^{-1} mode of R6G (Figure 3b) is dominated by a single peak at the fundamental transition and exhibits a transition amplitude ratio of 4.9:1. The 1504 cm^{-1} mode of R6G (Figure 3c) exhibits an increase in SER intensity at the 0–1 transition, corresponding to a transition amplitude ratio of 3.0:1. The surface-enhanced REP for the 1647 cm^{-1} mode of R6G (Figure 3d) contains appreciable contributions from both transitions, corresponding to a transition amplitude ratio of 1.1:1. The results presented in Figure 3 are in agreement with the REPs for R6G predicted by Shim et al.¹²

In addition, Figure 3c–d demonstrate a sharp increase in intensity in the region $< 18\,000 \text{ cm}^{-1}$. Since the surface-enhanced REP of R6G contains contributions from the resonance Raman effect, as well as EM enhancement and other surface effects, it is possible that this feature is attributable to surface effects. To test this hypothesis, a control experiment was performed using the nonresonant molecule benzenethiol (data not shown). The surface-enhanced REP of benzenethiol, which originates solely from EM enhancement and other surface effects, exhibited equivalent behavior to R6G in the region of interest. Therefore, the intensity observed $< 18\,000 \text{ cm}^{-1}$ (Figure 3c–d) is attributed to EM enhancement and surface effects. This hypothesis is consistent with the observation that the surface-enhanced REP of the largest Raman shift (1647 cm^{-1}) exhibits the sharp increase in intensity prior to that in the surface-enhanced REP for 1504 cm^{-1} , a feature that is not observed at

all in the 610 cm^{-1} data. Specifically, the AgIF substrates contain a distribution of enhancing features and those with plasmon resonances $\sim 600 \text{ nm}$ produce the largest EF.³¹ Therefore, modes with the largest Stokes shift will experience the surface plasmon enhancement first (i.e., at the lowest energy), and the sharp increase in intensity is observed for the higher-energy modes before the lower-energy modes. Presumably, if the laser is tuned far enough to the red, a similar increase for the 610 cm^{-1} mode would become apparent. Since the excitation profile $< 18\,000 \text{ cm}^{-1}$ is obscured by EM enhancement, only data $> 18\,000 \text{ cm}^{-1}$ were considered in the vibronic analysis.

Single-Molecule Surface-Enhanced REP of R6G. Single-molecule junctions were identified using the isotope-edited approach described previously.⁴ Briefly, SMSERS active sites were identified by eye and analyzed for the vibrational signature of only the R6G (R6G- d_0) isotopologue in order to provide direct comparison to ensemble-averaged measurements. The surface-enhanced resonance Raman spectrum of an individual R6G molecule on a Ag nanoparticle aggregate is presented in Figure 2b. The spectrum was obtained using 532-nm excitation from a frequency-doubled optical parametric oscillator ($P_{\text{ex}} = 0.050 \text{ W} \cdot \text{cm}^{-2}$, $t_{\text{ac}} = 10 \text{ s}$) at grazing incidence. The SMSER spectrum is consistent with the ensemble-averaged SER spectrum. However, wider Raman modes are observed in the single-molecule spectrum relative to the ensemble-averaged spectrum due to the relative bandwidths of the excitation sources.

The surface-enhanced REPs of an individual R6G molecule under dry N_2 are presented in Figure 4. Error bars represent one standard deviation from the mean, obtained from multiple measurements at each excitation energy. The data were fit to single Lorentzian functions, consistent with the expectations of a single-molecule measurement, as follows. Best fit to the data for the 610 cm^{-1} mode (Figure 4a) corresponds to $E_{\text{max}} = 18562 \text{ cm}^{-1}$ (538.7 nm) and fwhm = 365 cm^{-1} . For the 1504 cm^{-1} mode (Figure 4b) $E_{\text{max}} = 18561 \text{ cm}^{-1}$ (538.7 nm) and fwhm = 451 cm^{-1} . Finally, the 1647 cm^{-1} mode (Figure 4c) was fit to a single Lorentzian function with $E_{\text{max}} = 18598 \text{ cm}^{-1}$ (537.7 nm) and fwhm = 463 cm^{-1} . Overall, the linewidths of the single-molecule surface-enhanced REPs are narrower than the analogous ensemble-averaged linewidths, as expected.^{32,33} Whereas ensemble-averaged measurements are inhomogeneously broadened due to a distribution of local environments and are typically described by Gaussian distributions, the corresponding single-molecule measurements are narrower. The vibronic sideband (i.e., $E_{\text{max}} = 19246 \text{ cm}^{-1}$) corresponding to the 0–1 transition present in the ensemble-averaged data was not observed in the single-molecule surface-enhanced spectra likely due to two factors: (1) low signal-to-noise in this regime and (2) low data point density due to experimental limitations from commercially available filters (see Experimental Section). However, vibronic coupling of higher frequency modes to the 0–1 transition is supported by previous work, where surface-enhanced Raman spectra obtained at 514.5-nm excitation demonstrate that higher-frequency modes (e.g., 1647, 1504 cm^{-1}) are more intense relative to low-frequency modes (e.g., 610 cm^{-1}).⁹

(31) Schatz, G. C.; Van Duyne, R. P. *Electromagnetic Mechanism of Surface-Enhanced Spectroscopy*. In *Handbook of Vibrational Spectroscopy*; Chalmers, J. M., Griffiths, P. R., Eds.; Wiley: New York, 2002; Vol. 1, pp 759.

(32) Myers, A. B. *Annu. Rev. Phys. Chem.* **1998**, *49*, 267.

(33) Moerner, W. E.; Kador, L. *Phys. Rev. Lett.* **1989**, *62*, 2535.

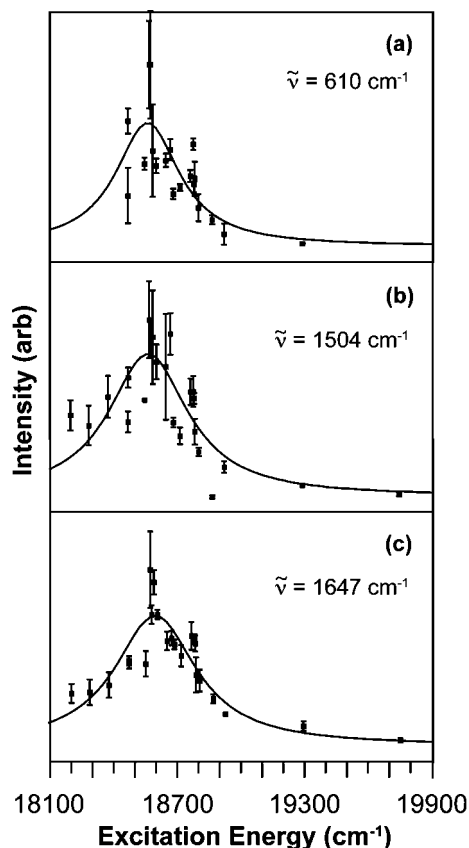


Figure 4. Single-molecule surface-enhanced resonance REPs of different Raman modes for an individual R6G molecule on colloidal silver. (a) $\nu = 610$, (b) 1504 , and (c) 1647 cm^{-1} ($P_{\text{ex}} = 0.050\text{ W}\cdot\text{cm}^{-2}$, $t_{\text{ac}} = 10\text{ s}$). Error bars represent one standard deviation from the mean obtained from multiple measurements at each excitation wavelength. The data were fit to single Lorentzian functions (solid lines) with linewidths on the order of 400 cm^{-1} .

Upon closer inspection of the data presented in Figure 4, we considered that fine structure on the order of 100 cm^{-1} may be observed due to vibronic coupling or EM enhancement effects. Vibronic coupling is known to impart structure to both absorption and emission spectra.³⁴ Consequently, fluorescence spectroscopy provides insight to the structure and linewidths in resonance REPs.²⁷ On pyrolytic graphite surfaces, single R6G molecules exhibit vibronic structure on the order of $\sim 1145\text{ cm}^{-1}$ and homogeneous linewidths of $\sim 450\text{ cm}^{-1}$.³⁵ The single-molecule fluorescence spectra of rhodamine 630, a R6G structural analogue, in a polymer matrix revealed comparable values of ~ 1145 and $\sim 450\text{ cm}^{-1}$, respectively.³⁶ In both cases the homogeneous line width, a consequence of pure dephasing,³² prohibits the observation of structural features $< 500\text{ cm}^{-1}$. Instead, these studies are in agreement with the fwhm observed in our single-molecule surface-enhanced REPs considering single Lorentzian fits (i.e., 365 , 451 , and 461 cm^{-1}).

Both resonance Raman and EM enhancement effects contribute to the surface-enhanced REPs (i.e., $\text{EF}_{\text{total}} = \text{EF}_{\text{RR}}\text{EF}_{\text{SERS}}$).³⁷ Therefore, an alternative explanation for the apparent fine structure in the single-molecule surface-enhanced REPs is

that EM enhancement in the hot spot may fluctuate as a function of excitation energy, manifesting as fine structure atop the homogeneously broadened single-molecule surface-enhanced REP. To explore the role of EM enhancement in the single-molecule surface-enhanced REPs, we performed a series of DDA calculations on a model T-shaped SMSERS aggregate inspired by previous experiments¹³ as a function of excitation energy. The results of our calculations are shown in Figure 5a and demonstrate that EM enhancement in the hot spot does not fluctuate on sub-nanometer ($\sim 9\text{ cm}^{-1}$) increments over a 200 cm^{-1} range (centered at $\sim 18\,775\text{ cm}^{-1}$) and exhibit a gradual downward slope. In fact, EM enhancement is only modestly changed over the excitation bandwidth of the experiment (Figure 5a, inset). The location of the hot spot was also found to be invariant with respect to excitation wavelength. Moreover, we previously demonstrated that EM enhancement roughly tracks the extinction spectrum of the model T-shaped aggregate.¹³ The resonant Rayleigh scattering spectrum for the nanoparticle aggregate used in the SMSERS study is presented in Figure 5b.³⁸ Although features are present in the scattering spectrum, they are too broad to impart fine structure on the single-molecule surface-enhanced REPs. In fact the scattering peaks are broader ($> 2000\text{ cm}^{-1}$) than the excitation profile ($\sim 400\text{ cm}^{-1}$) indicating that the shape of the single-molecule surface-enhanced REPs is dominated by the properties of the molecule (i.e., resonance Raman effects). Considering the aforementioned single-molecule fluorescence studies and the weak wavelength-dependence of EM enhancement, the apparent fine structure in the single-molecule surface-enhanced REPs is attributed to artificial effects (e.g., irreproducible alignment, noise, and small environmental fluctuations).

Figure 6 presents a comparison of the single-molecule surface-enhanced REP to the ensemble-averaged surface absorbance of R6G. The single-molecule data are an integration of all vibrational modes from $\sim 500\text{--}1800\text{ cm}^{-1}$, with error bars representing one standard deviation from the mean. The total single-molecule surface-enhanced REP is well described by a single Lorentzian with best fit corresponding to $E_{\text{max}} = 18563\text{ cm}^{-1}$ (538.7 nm) and $\text{fwhm} = 449\text{ cm}^{-1}$. The fwhm of the single-molecule data is substantially narrower than the surface absorbance, consistent with a reduction to inhomogeneous broadening. Moreover, the maximum of the single-molecule data ($E_{\text{max}} = 18563\text{ cm}^{-1}$) is consistent with the 0–0 transition of the surface absorbance ($E_{\text{max}} = 18409\text{ cm}^{-1}$). The deviation from the ensemble average is significant, demonstrating the existence of single-molecule resonance Raman, as well as the utility of single-molecule measurements.

The experiments presented in this manuscript are aimed at understanding the contributions of the resonance Raman and EM enhancement effects to the SMSERS mechanism as a function of excitation frequency. It has been previously established that at 532-nm excitation, single-R6G sensitivity is achievable due to three effects, (1) a large preresonant Raman cross-section of R6G (10^{-26} cm^2 at 633 nm),¹⁴ (2) a resonance Raman contribution of $10^3\text{--}10^4$ (cross-section is 10^{-23} at 532 nm),¹² and (3) the 10^8 EM contribution from the nanoparticle aggregate.¹³ Here, we have addressed the question how the single-molecule EF_{total} changes about the molecular resonance using a finely tunable excitation source. The structure of the

(34) Valeur, B. *Molecular Fluorescence: Principles and Applications*; Wiley-VCH: New York, 2002.

(35) Uehara, Y.; Ushioda, S. *Appl. Phys. Lett.* **2005**, *86*, 3.

(36) Weber, M. A.; Stracke, F.; Meixner, A. J. *Cytometry* **1999**, *36*, 217.

(37) Zhao, J.; Dieringer, J. A.; Zhang, X.; Schatz, G. C.; Van Duyne, R. P. *J. Phys. Chem. C* **2008**, *112*, 19302.

(38) The structure of the nanoparticle aggregate used in this study was not characterized by correlated high-resolution transmission electron microscopy. However, previous work in ref 13 suggests that the EM enhancement tracks the scattering spectrum.

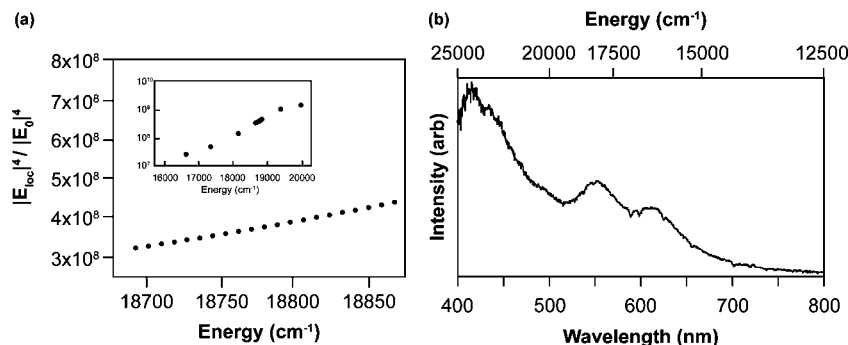


Figure 5. (a) Electromagnetic enhancement calculated as a function of excitation energy in 0.5-nm increments from a model T-shaped nanoparticle aggregate inspired by previous experiments.¹³ (inset) Calculated electromagnetic enhancement for the full range of the experiment. E_0 and E_{loc} are the incident and local electromagnetic fields, respectively. (b) Resonant Rayleigh scattering spectrum of the nanoparticle aggregate used in the SMSERS study (corresponding Raman data shown in Figures 2b, 4, and 6).

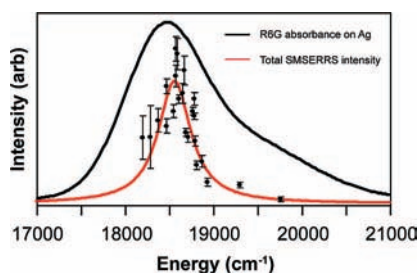


Figure 6. Comparison of the single-molecule surface-enhanced resonance Raman (SMSERS) intensity (red line with points) to the ensemble-averaged surface absorbance spectrum on Ag. The single-molecule REP (points) was obtained from the sum of all observed Raman modes and was fit to a Lorentzian function (red solid line) where the error represents one standard deviation from the mean ($E_{max} = 18563 \text{ cm}^{-1}$ and $fwhm = 449 \text{ cm}^{-1}$). The molecular absorbance of R6G on 200 nm Ag film (black) was fit by a sum of two Gaussians. As expected, the single-molecule data are significantly narrower than the ensemble-averaged analogue ($\sim 1100 \text{ cm}^{-1}$).

single-molecule surface-enhanced REPs is dominated by the resonance Raman enhancement while the magnitude is dominated by electromagnetic enhancement, an observation that is supported by DDA calculations (Figure 5). Moreover, the computations reveal that the EM enhancement is $> 10^7$ over a wide range of excitation frequencies, promising for SMSERS detection over a large excitation bandwidth. In fact, off molecular resonance (633-nm excitation), the resonance Raman enhancement is small and in order to observe single molecules, Le Ru et al. employed higher laser intensities to compensate for diminished resonance enhancement.¹⁴

Conclusion

Surface-enhanced Raman spectra were collected from individual and ensembles of R6G molecules as a function of excitation frequency. The ensemble-averaged surface-enhanced REPs are well described by a sum of two Gaussians, corresponding to the 0–0 and 0–1 vibronic transitions that are derived from a deconvolution of the molecular absorbance spectrum on Ag. The relative ratios of the 0–0 and 0–1

transitions varies with vibrational frequency, in agreement with recent predictions.¹² These results highlight the role of excitation energy in determining resonance Raman intensities for R6G on surface-enhancing nanostructures. Single-molecule surface-enhanced REPs were measured about the molecular resonance of R6G using a tunable excitation source. Consistent with the expectations for single-molecule behavior, the narrow profiles were fit to single Lorentzian functions dominated by homogeneous broadening. The fwhm of the single-molecule surface-enhanced REPs were measured to be $\sim 400 \text{ cm}^{-1}$. Overall, the linewidths of the single-molecule surface-enhanced REPs are narrower than the analogous ensemble-averaged linewidths, as expected due to a reduction in inhomogeneous broadening. To our knowledge, this work demonstrates the first single-molecule surface-enhanced REP with high data density across the molecular resonance. Future directions include (1) experimentally characterizing the wavelength dependence of the EM enhancement in a well-defined single-molecule hot spot, (2) probing the distribution of single-molecule surface-enhanced REPs, and (3) SMSERS experiments on nonresonant molecules with an eye toward sensing and detection applications. A large set of single-molecule surface-enhanced REPs and the contributing nanostructure properties (e.g., LSPR scattering, morphology, chemical composition) can reveal the effects of local environment on energy, linewidth, and population distribution, information otherwise hidden under the ensemble. Fundamental investigations such as the work presented herein will provide valuable insight for the challenge of achieving broad application of the SMSERS technique.

Acknowledgment. This work was supported by the NSF (EEC-0118025, CHE-0414554, BES-0507036), the AFOSR DURIP (FA-9550-07-1-0526), DTRA JSTO (FA9550-06-1-0558), AFOSR/DARPA Project BAA07-61 (FA9550-08-1-0221), the NSF NSEC program (EEC-0647560), and the NSF MRSEC (DMR-0520513) at the Materials Research Center of Northwestern University.

JA8080154